NASA CONTRACTOR
REPORT

NASA CR-120509

(NASA-CR-120509) FLIGHT/GROUND SAMPLE COMPARISON RELATING TO FLIGHT EXPERIMENT M552, EXOTHERMIC BRAZING (Wisconsin Univ.) 40 p HC $3.75 CSCL 13H

N75-10969

Unclas
G3/12 53895

FLIGHT/GROUND SAMPLE COMPARISON RELATING TO FLIGHT EXPERIMENT M552, EXOTHERMIC BRAZING

By Richard W. Heine, Clyde M. Adams, and
Thomas A. Siewert
University of Wisconsin
Department of Metallurgical and Mineral Engineering
Madison, Wisconsin 53706

December 1973

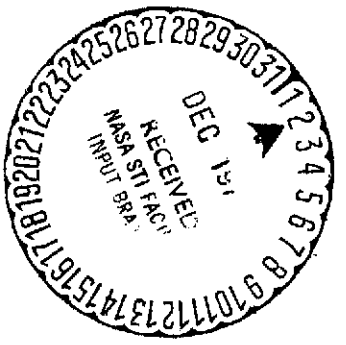

Prepared for

NASA-GEORGE C. MARSHALL SPACE FLIGHT CENTER
Marshall Space Flight Center, Alabama 35802

TECHNICAL REPORT STANDARD TITLE PAGE

1. REPORT NO.	2. GOVERNMENT ACCESSION NO.	3. RECIPIENT'S CATALOG NO.
NASA CR-120509		

4 TITLE AND SUBTITLE	5. REPORT DATE
Flight/Ground Sample Comparison Relating to Flight Experiment M552, Exothermic Brazing	December 1973
	6. PERFORMING ORGANIZATION CODE

7. AUTHOR(S)	8. PERFORMING ORGANIZATION REPORT #
Richard W. Heine, Clyde M. Adams, Thomas A. Siewert	

9. PERFORMING ORGANIZATION NAME AND ADDRESS	10. WORK UNIT NO.
University of Wisconsin Department of Metallurgical and Mineral Engineering Madison, Wisconsin 53706	11. CONTRACT OR GRANT NO. NAS 8-28733
	13. TYPE OF REPORT & PERIOD COVERED

12. SPONSORING AGENCY NAME AND ADDRESS	
National Aeronautics and Space Administration Washington, D. C. 20546	Contractor Report
	14. SPONSORING AGENCY CODE

15. SUPPLEMENTARY NOTES

16. ABSTRACT

Comparisons have been made between Skylab and ground-based specimens of nickel and stainless steel which were vacuum brazed using silver-copper-lithium alloy with various joint configurations. It was established the absence of gravity greatly extends the scope of brazing since capillary flow can proceed without gravity interference. There was also evidence of enhanced transport, primarily in that liquid silver copper alloy dissolves nickel to a much greater extent in the zero gravity environment.

17. KEY WORDS	18. DISTRIBUTION STATEMENT
	Unclassified - Unlimited W.K. Vaudaman

19. SECURITY CLASSIF. (of this report)	20. SECURITY CLASSIF. (of this page)	21. NO. OF PAGES	22. PRICE
Unclassified	Unclassified	40	NTIS

For sale by National Technical Information Service, Springfield, Virginia 22151

TABLE OF CONTENTS

PRECEDING PAGE BLANK NOT FILMED

INTRODUCTION

Detailed examinations using a variety of observational and analytical techniques were conducted on exothermically brazed Skylab specimens and compared with substantially identical specimens brazed on earth. The thermal, physical, chemical and dimensional features of the various specimen materials and designs were replicated as closely as possible to insure that the only significant difference between a particular Skylab specimen and its ground characterization counterpart was the presence or absence of gravity. For each Skylab specimen there were three corresponding ground characterization specimens. Similarities and differences were observed in metallographic structure, distribution of alloying elements, and phase boundary contours, and these have been interpreted primarily to identify specific effects of zero gravity environment on transport, solidification, and phase configuration. While there has been a natural tendency to emphasize differences and unique effects of zero gravity, of equal importance are similarities, i.e. physical and metallurgical features exhibiting almost total insensitivity to the presence or absence of gravity.

MATERIALS, DIMENSIONS AND ENVIRONMENTS

The solid materials being brazed were tubular sections of 304L stainless steel and pure nickel. The brazing alloy was a eutectic composition mixture of silver and copper (72% silver, 28% copper) containing a small concentration (0.5%) of lithium. There were four specimen designs in which the most important variations were in the composition of the solid (stainless or nickel) and dimensions of the capillary gap between the inner tubular section and the concentric outer sleeve. In all specimens the silver-copper braze alloy was preplaced in ring-grooves situated for that purpose, one at each end of the specimen. Upon melting, flow of the liquid silver-copper alloy into the gap was under the impulsion of capillary action, in which the force producing flow is primarily surface tension. Gravity, when present, has a modifying effect on the surface tension force field which may or may not be negligible, depending on the magnitude of the capillary gap. The four specimen designs are listed below:

0.005" - Gap - 304L Material
SLS1 - Skylab Flight Specimen
MCS-1, 2 & 3 - Ground Characterization Specimens

0.010" - Gap - Pure Nickel
SLN2 - Skylab Flight Specimen
MCN-1, 2 & 3 - Ground Characterization Specimens

0.020" - Gap - 304L Material
SLS3 - Skylab Flight Specimen
MCS-4 - 5 & 6 - Ground Characterization Specimens

0.000" - 0.030" Taper Gap - Pure Nickel Material
SLN4 - Skylab Specimen
MCN-4, 5 & 6 - Ground Characterization Specimens

The findings reported in the following paragraphs evolved primarily from brazed stainless steel samples SLS 3, and MCS 4, 5, and 6, and brazed Ni samples SLN 4 and MCN 4, 5, and 6. These have been referred to as "wide gap" samples, because, to develop effective capillary flow on earth using these materials, gap clearances are generally held below 0.005 inch. One objective which influenced specimen design was to observe wide-gap capillary flow in the absence of gravity.

The other eight specimens (SLS 1 and MCS 1, 2, and 3 and SLN 2 and MCN 1, 2, and 3) incorporated narrower capillary gaps and have been examined at the Battelle Memorial Institute.

Solid exothermic heat sources, identical as nearly as possible from specimen to specimen, duplicates of which were thermally, statistically and analytically characterized at M. I. T., were used for all brazing experiments; the thermal regime and reproducibility of the exothermic heat source have been well-documented.

The Skylab as well as the ground characterization specimens were brazed in vacuo the order of 10^{-4} - 10^{-5} Torr. The objective of replicating the environment between the Skylab and ground characterization specimens in all particulars except gravity, seems to have been fulfilled quite satisfactorily. There is one additional field effect which may be significant, namely, that the Skylab specimens unavoid ably traveled at high speed through the earth's magnetic field.

PHASE RELATIONSHIPS

The pertinent binary equilibrium systems, copper-nickel, silver-copper, and silver-nickel, are well established but the ternary system, silver-copper-nickel, is not known with precision. Copper and nickel are mutually completely soluble in both the liquid and solid states; silver and copper exhibit complete liquid but limited solid solubility; silver and nickel exhibit very limited mutual solubility in both

the liquid and solid states. The one published study of the ternary system suggests that silver-copper alloys rich in silver exhibit very limited capacity for dissolving nickel except at very high temperature[1]. Alloy element distributions observed in both the Skylab and ground characterization specimens exhibit appreciable concentrations of nickel in the solidified braze alloy. Moreover, much more nickel dissolved in the Skylab specimens than in the ground-based specimens.

The binary silver-copper alloy without nickel separates upon solidification into two solid phases, one rich in copper but containing some dissolved copper. When nickel is added to the silver-copper alloy, upon solidification the nickel preferentially associates with the copper-rich phase, being quite insoluble in the silver-rich phase. Moreover, silver and nickel appear to be mutually exclusive in the copper-rich phase. In fact, two kinds of copper-rich phase form, one which contains nickel but no silver, and the other which contains silver but almost no nickel. The solidification process is rendered quite complicated by the addition of nickel. The simple binary 72% silver 28% copper freezes substantially at one temperature, 780°C, and the product of solidification exhibits the classical eutectic structure, a finely dispersed mechanical mixture of silver-rich and copper-rich phases. The presence of nickel increases the temperature at which solidification begins, and the first solid crystals which form contain copper and nickel with practically no silver. These crystals become fairly large before the rest of the alloy freezes at about 780°C. These large copper-nickel crystals or dendrites are called primary because they form first upon cooling. Both the ground characterization and Skylab specimens of brazed nickel exhibited this characteristic structural feature. Some primary copper-rich dendrites were also observed in the stainless steel specimens, but these contained much less nickel, because stainless only contains 8% nickel. As more and more nickel dissolves in the silver-copper alloy, the fine eutectic structure progressively, and finally completely, disappears. Very abnormal structures, surprisingly high in nickel concentration, were observed only in the Skylab samples. The identification of these abnormal structures with high nickel concentration is still somewhat circumstantial; the important question is: Is the structure abnormal because of the absence of gravity, or is the structure abnormal because so much nickel has dissolved? And further, did more nickel dissolve because of the absence of gravity? At this stage of the study it appears that the increased nickel concentration in the Skylab specimens accounts for the abnormal structure.

The presence of dissolved nickel in the liquid silver-copper alloy has a subtle but logical effect on the formation of primary phases. In the absence of nickel, solidification of the 72% silver 28% copper substantially begins and ends at 780°C, and the structure produced is a finely dispersed classical eutectic mixture of silver-

rich and copper-rich phases. The first effect of dissolved nickel is to increase the temperature at which solidification begins: A copper-rich primary phase, containing nickel, forms at a temperature well above 780°C. Upon cooling, when the temperature begins to approach 780°C, virtually all the nickel has been rejected from the liquid solution, because the nickel is virtually insoluble in the silver-rich liquid at temperatures below 850°C. Thus, it is the nickel which causes the primary copper phase to form at a relatively high temperature; however, this primary crystallization has the effect of removing copper from the liquid. The remaining liquid contains appreciably more than 72% silver, and primary silver-rich phase now must form at a temperature about 780°C. When the eutectic temperature, 780°C, is finally reached, whatever liquid still remains contains very nearly 72% silver-28% copper, and freezes to a fine eutectic structure. If the initial nickel concentration in the liquid is high enough, solidification will become nearly complete at a temperature above 780°C, and no normal eutectic structure will form. "The two-phase field resulting from the silver-copper eutectic decomposition terminates with the addition of 5 wt % Ni."[5] The quotation is an interpretation of early work done on the silver-copper-nickel ternary system[1], and is qualitatively correct. The limiting value of 5% nickel, in light of the present study, appears to be somewhat low; the actual value is probably closer to 10% nickel.

TRANSPORT

Both Skylab nickel specimens (the one examined at Battelle and the other at the University of Wisconsin) exhibited appreciably higher concentrations of dissolved nickel in the braze alloy than did any of the ground characterization specimens. Several explanations, most of them unreasonable, may be hypothesized. It seems very unlikely that the absence of gravity would materially influence either the solubility or the diffusivity of nickel in a silver-rich liquid. In fact, the combinations of time, temperature, and liquid state diffusivity, and the dimensions of the capillary space in the nickel specimens, are such that diffusion cannot be the limiting factor. Even with the wide (0.020 inch) gap nickel specimen, the time, t, required for nearly complete diffusion throughout the capillary section can be estimated from:

$$t = \frac{0.2L^2}{D}$$

where $L = 0.020" = 0.051$ cm., gap clearance

$D = 2.8 \times (10)^{-5}$ cm^2/sec [2, 3], diffusivity in liquid silver at 1000°C

$t = 18$ seconds

This specimen is obviously at elevated temperature much longer than 18 seconds. If diffusion is augmented by convection, the time becomes even less. However, the transport situation is evidently complicated enough that it has not yet proven possible to establish a good analytical representation. It does seem that convection has an effect on transport at the interface between the solid nickel and the braze alloy. In both the ground characterization and Skylab specimens, there develops a layer of copper-nickel alloy at this interface. In the absence of convection, this layer develops sufficient thickness to act as an effective diffusion barrier. Weighing all the facts and observations, it seems likely convection was more vigorous in the Skylab than in the ground characterization specimens. The interface structure reflects this; there is a distinct tendency for the copper nickel interface layer to be thinner in the Skylab than in the ground characterization specimens. This is not uniformly true, in fact, the observation must be and has been made statistically by close scrutiny of many portions of the interface on each specimen.

In summary, the present conclusion is there was sustained convection after capillary flow in the Skylab specimens which was sufficiently vigorous to prevent development of an effective copper-nickel alloy diffusion barrier. It is postulated this sustained convection may have resulted from the interaction of the traveling Skylab specimens with the earth's magnetic field.

STRUCTURE AND COMPOSITION

A. Nickel Specimens

In Figures 1, 2 and 3 are shown photomicrographs of structures found within the capillary brazed joint in specimen SLN 4. These structures are normal in most respects, being almost identical to corresponding sections taken from the ground characterization sample (Figure 4). The fine eutectic mechanical mixture occupies most of the field of view. The large dark regions are copper-rich and contain some nickel but almost no silver. The small dark regions are copper-rich and contain some silver but very little nickel. The white regions are silver-rich, containing some copper but essentially no nickel. In the Skylab specimens there occasionally appears a relatively large primary silver-rich dendrite; this has never been observed in any of the ground characterization specimens, and is an indirect result of high nickel concentration.

The alloy element distribution is typified in Figures 5, 6 and 7 which are, respectively, electron microprobe area scans showing nickel, copper, and silver distributions in the same field of view shown in Figure 4. In particular, it can be seen the large copper-rich

dendrites contain copper and nickel but essentially no silver, and the small dark areas (sometimes referred to as secondary copper-rich phase) are rich in copper but contain no nickel. This pattern of alloy element distribution is repeated throughout in both the Skylab and ground characterization specimens, and supports the statement made above that silver and nickel are substantially mutually exclusive in the copper-rich phase, a feature which complicates the solidification sequence. Measurements were made of a structural feature called dendrite arm spacing. In the tree-like growth of dendrites, there occur regions in which the arms of the dendrites are quite regularly spaced, and it has been found this spacing depends systematically on alloy composition and the cooling rate which prevailed during solidification. Dendrite arm spacings were found to be the same in the Skylab as in the ground characterization specimens, as had been expected. A typical view permitting measurement of dendrite arm spacing is shown in Figure 8, where the spacing is consistent with a dendrite containing 10% nickel 90% copper which solidified at a cooling rate of about 50°C per minute(4).

The structures observed in the nickel Skylab specimens have been characterized as normal, abnormal and mixed. These structures are shown in Figures 9 through 12. Figure 9, from Skylab sample SLN 4 shows the normal structure, which is to say it is substantially identical in all important features to the brazed nickel ground characterization specimens. There are occasional large nickel-containing, copper-rich, silver-free dendrites to be found throughout the braze alloy. Then, near the interface, there are peninsular protuberances, epitaxial with the solid nickel, which are also rich in copper with appreciable concentrations of dissolved nickel. The rest of the structure is the fine eutectic mixture of silver-rich (white) solid solution containing relatively small particles of copper-rich, silver-bearing, low-nickel solid solution. A detailed microprobe survey of this structure gave the following results?

(1) Near the center of a large dendrite the composition is 20% nickel 80% copper.

(2) Near one of the tips of the same large dendrite the composition is 10% nickel 90% copper.

This alloy distribution is consistent with the nature of dendrite growth. The first material to form upon cooling has the highest nickel content, and then, as the crystals grows, the exterior regions exhibit progressively lower nickel concentrations, and form at progressively lower temperatures. This is often referred to as a cored structure. The proturbances growing from the brazed nickel interface also present a logical variation in composition.

(3) In the protuberance, very near the original interface, the composition is 35% nickel 65% copper.

(4) Halfway out to the tip the composition is 20% nickel 80% copper.

(5) At the tip the composition is 10% nickel 90% copper, the same as the tip of a large dendrite.

The small copper-rich particles within the finely dispersed eutectic structure contain something less than 10% nickel.

The abnormal structure is shown in Figure 10. There is a complete absence of the typically fine eutectic dispersion, and the relatively large dark particles contain nickel concentrations which range from about 40% nickel in their centers down to about 25% nickel near their exterior boundaries. These particles are therefore cored, but do not exhibit the usual morphology of dendrites. The total nickel concentration in the field of view shown in Figure 10 is quite high, estimated close to 10% nickel overall. Furthermore, the probe shows that the layer of nickel-copper alloy at the braze-nickel interface is quite thin compared to corresponding locations on ground characterization specimens. The thinner this layer the less effective it is as a diffusion barrier. Since it is unlikely any of these specimens reached temperatures much above 1000°C, the high nickel concentration is surprising in that it appears to exceed the maximum solubility which can be inferred from the published information on the ternary silver-copper-nickel system[1].

Figures 11 and 12 show mixed normal and abnormal structures. Figure 11 happens to be from a ring-groove location, where the cross-section of the braze alloy is relatively large, and Figure 12 shows a region within the capillary gap. All three structures, normal, abnormal and mixed, are found at various locations throughout the specimen; there is no systematic dependence on location.

B. Stainless Specimens

Abnormal and mixed structures were not observed in any stainless steel specimens, presumably because the stainless, containing only 8% nickel, does not introduce enough nickel into liquid solution to modify eutectic solidification appreciably. Within the capillary gap in the stainless Skylab specimens, there is a pronounced tendency for primary silver-rich dendrites to form, clearly shown in Figures 13 and 14. In fact, in these regions there has been some impoverishment in copper, apparently by dissolution into the stainless; the copper is soluble in the solid stainless, whereas silver is not. However, primary silver-rich phase has never been observed in the ground characterization specimens. This is yet further evidence for enhanced transport in the Skylab specimens, which must, for reasons already stated, relate to convection, i.e. convective disturbance overcomes any tendency for an effective diffusion barrier to form at the liquid-solid

interface. In the ring-groove of the stainless Skylab specimen, the structure is identical to that in the ground characterization specimens, exhibiting primary copper-rich dendrites, containing generally about 2% nickel (sometimes less), surrounded by normal finely dispersed eutectic structure (see Figure 15).

For comparison, structures observed in stainless ground characterization specimens are shown in Figures 16 and 17; these exhibit primary copper-rich phase together with normal eutectic. In the stainless Skylab specimen, primary silver-rich but no primary copper-rich phase is observed in the capillary gap, and primary copper-rich but no silver-rich phase was observed in the ring-groove location. In the nickel Skylab specimen, primary silver-rich and copper-rich phases were frequently observed together (Figures 1 and 2), both primary phases resulting from the presence of nickel dissolved in the liquid prior to solidification.

Another curious feature of the stainless Skylab specimen was the presence of finely dispersed stainless steel particles within the braze alloy. The first inclination is to attribute these particles to the presence of debris remaining from machining the specimens. However, the specimens were very thoroughly cleaned, and the particles are extremely small, ranging from 0.5 to 5.0 microns (micrometers) in diameter. Stainless does not readily fragment into such fine particles; it is more likely these inclusions, shown in Figures 18 and 19, are the consequence of erosive attack of the stainless by the liquid metal. This is taken as still further evidence of vigorous convection peculiar to the Skylab specimens, because these particles were not detected in any of the ground characterization specimens.

Summarizing, the results of examining the stainless steel Skylab and ground characterization specimens have revealed significant differences and similarities. The formation of primary copper-rich dendrites and normal fine eutectic structure was observed in all stainless specimens in the groove location. The stainless Skylab specimens was distinguished by the presence of primary silver-rich phase and non-uniform dispersion of very fine stainless steel particles within the braze alloy.

SURFACE TENSION EFFECTS

An observation of major importance is that true capillary flow can be developed in wide-gap apertures when gravity is absent. This had been predicted, and was a reason for inclusion of wide-gap specimens (SLS 3, 0.020 inch gap and SLN 4, tapering to 0.030 inch gap).

There are practical as well as scientific implications to wide-gap capillary behavior. One principal consequence is that brazing, as a means for joining materials, is a much more versatile process in zero gravity space environment than it is on earth. Commercial terrestrial capillary brazing is limited by gravity interference to gap clearances rarely exceeding 0.005 inch, which imposes serious constraints on machining and fixturing. The absence of the need for close clearances and relatively smooth parallel surfaces, as required on earth, greatly extends the applicability of brazing as contrasted, for example, with welding, fastening, or other joining techniques, when structural fabrication is to be done in space environment.

Stainless Skylab specimen SLS 3, with a uniform 0.020 inch capillary gap, developed what in brazing parlance would be referred to as a "starved" joint; there was not enough braze alloy completely to fill the gap. Of course, it was not a primary objective of the experiment to produce high quality brazed joints; examination of the "starved" joint was much more informative than would have been the case had excess braze alloy been provided. The liquid metal preferentially migrated to positions of minimum gap clearance, as is shown quite clearly in Figure 20. (The gap variation resulted from slight deformation due to thermal stresses imposed during heating.) But the significant point is capillary flow in the wide gap was quite complete. The corresponding ground characterization specimens (MCS 4, 5 and 6) exhibited pronounced gravity interference with capillary flow.

The contribution of gravity to the flow of liquid in small apertures can be assessed quantitatively: The vapor-liquid phase boundary, or meniscus, which develops at the extremity of a layer of liquid reposing in a capillary gap, exerts a force on the liquid. This force results in a pressure difference across the meniscus surface. Since the meniscus is generally concave, the pressure within the liquid is lower than that in the vapor, near the meniscus. This pressure difference can be compared to the pressure difference prevailing on earth within the liquid due to gravity, assuming some fixed vertical dimension for the liquid capillary. The ratio, R, of the gravitational pressure difference to the surface tension pressure difference is given by:

$$R = \frac{\rho g Z L}{2\sigma}$$

where ρ = density of liquid, 9.2 gm/cm^3 for liquid silver

g = 980.7 cm/sec^2, acceleration due to gravity on earth

Z = vertical height (on earth) of liquid capillary under consideration, here taken arbitrarily as 2 cm.

L = magnitude of capillary gap (clearance between parallel flat surfaces) in cm.

σ = liquid-vapor surface tension (liquid-vapor interfacial energy) taken as 900 dyne/cm[6], [7] for silver-rich liquid.

The above relationship can be used to express gravitational pressure difference as a percent of the pressure difference induced by surface tension:

Joint clearance (inches)	Gravitational pressure differences (% of surface tension pressure difference)
0.002	5
0.005	13
0.010	25
0.020	51

Practical capillary brazing on earth is limited to a gravitational contribution generally less than 10%; hence, joint clearances rarely exceed 0.005 inch.

Some general characteristics of capillary flow were manifest in a review of metal distribution in all M552 Skylab specimens. The pressure in liquid near a small gap meniscus is smaller than near a wide gap meniscus; therefore pressure differences develop in complex capillary systems tending to drive the liquid from wide gap to narrow gap locations. For example, when the braze gap was fairly narrow (SLS 1, 0.005 inch), the ring-grooves were almost drained of liquid; in a wide gap specimen (SLS 3, 0.020 inch), not only was the joint "starved" as mentioned above, but the wide gap was far less effective in draining liquid from the ring-grooves (thus contributing indirectly to the "starvation" of the joint). In consequence, an obervable, measurable meniscus developed in ring-grooves near wide gaps. For example, the upper ring-groove in specimen SLN 4 is near a very wide (0.030 inch) gap, which was incapable of withdrawing much liquid from the groove and the residual liquid formed the meniscus shown in Figure 21, according opportunity for observation of a radially symmetrical liquid-vapor surface contour in the absence of gravity. This contour has been found numerically consistent with the following equation which governs in the absence of gravity, provided the surface

tension is uniform from point to point on the meniscus surface.

$$\frac{dY}{dX} = \sqrt{\left(\frac{\sigma}{\Delta P}\right)^2 \left(\frac{2Y}{Y^2+C}\right)^2 - 1}$$

where Y = distance from the centerline of the specimen to a point on the meniscus, measured perpendicular to the centerline

X = distance measured parallel to the centerline from the center of the ring-groove

C = integration constant

σ = surface tension

ΔP = pressure difference prevailing across the meniscus surface (and constant from point to point along the meniscus surface)

The conformance of the meniscus surface with the equation supports the conclusion that the liquid-vapor surface tension is substantially uniform. This is of importance because the surface tension is quite sensitive to variations in temperature and surface composition.

CONCLUSIONS

The absence of gravity greatly extends the scope of brazing, and, thereby, the applicability of brazing to fabrication in space. In zero gravity environment, the surface tension forces begetting capillary flow are unfettered, while on earth these forces must compete with gravity. Study of braze alloy distribution in Skylab specimens clearly indicates that dimensional tolerances, especially braze gap clearances, will be far less critical to joining operations in space than on earth. The practical significance of this fact, which had been predicted but never tested, can hardly be overemphasized. In space fabrication, many joints, which on earth would be produced by welding, should probably be brazed.

The absence of gravity definitely and surprisingly changes the ways in which liquid and solid metals interact. For example, for the same time and temperature conditions of exposure (a) liquid silver-copper alloy dissolves nickel more rapidly in space than on earth, and

(b) solid stainless steel dissolves copper from liquid silver-copper alloy more rapidly in space than on earth. The detailed mechanisms by which these reactions are hastened have not been positively identified, and this effect of space environment had not been predicted. The space environment appears to offer unique advantages for implementation of some liquid-solid reactions, and also the measurement of solubilities. For example, the Skylab experience clearly indicates a higher solubility of nickel in liquid silver-copper alloy than had been found in the earth-bound studies; this is not because nickel is more soluble in space, but rather because it dissolves more rapidly. This pattern of behavior suggests that saturated liquid metal solutions can be more easily produced, and true solubilities more easily determined in space than on earth.

Liquid-vapor boundary surfaces (menisci), and the flow of liquid metal under the impulsion of surface tension forces, are in close conformance with what had been predicted for zero gravity environment. There were no unexplained effects, and, in the Skylab specimens, the surface tension of liquid silver-copper alloy appears to have been quite uniform.

The presence or absence of gravity has no observable effect on the mechanism of alloy solidification, Such microstructural details as dendrite configuration, and eutectic structure were the same in space as on earth.

FURTHER WORK

There were some pronounced and surprising effects of zero gravity space environment on migration of alloy elements during liquid-solid interaction. Detailed microchemical analyses, especially at and near phase boundaries, are of particular interest. These need to be done in far greater depth than has been possible to date. The value of the Skylab specimens is incalculable, and all possible information should be gleaned from them. An immediate objective would be to shed further light on why certain liquid-solid reactions, such as the dissolution of nickel take place more rapidly in space environment.

The Skylab experience provides clues to fruitful areas for further space research opportunities. The whole spectrum of liquid-solid reactions, not necessarily limited to metallic systems, should now come under consideration. It seems likely space will prove valuable as a polyphase processing, as well as a laboratory environment.

REFERENCES

1. W. Guertler and A. Bergmann, "Study of the Ternary Ag-Cu-Ni", Zeitschrifte fur Metallkunde, 25, 53 (1933).

2. L. Yang, S. Kado, and G. Derge, Trans. Metall. Soc. AIME, 221, 72 (1961).

3. V. G. Leak and R. A. Swalin, Trans. Metall. Soc. AIME, 230, 426 (1964).

4. L. Backerud and L. M. Liljenvall, "The Solidification Characteristics of 7 Constitutionally Different Types of Binary Copper Alloys, INCRA Project 165, Swedish Institute for Metal Research, Stockholm, 1971.

5. Metals Handbook, 8, 380 (1973).

6. U. S. Atomic Energy Comm. Publ., "Liquid Metals Handbook", Washington (1952).

7. F. Sauerwald, et al., Z. F. Anorg. Chem., 181, 353, (1929).

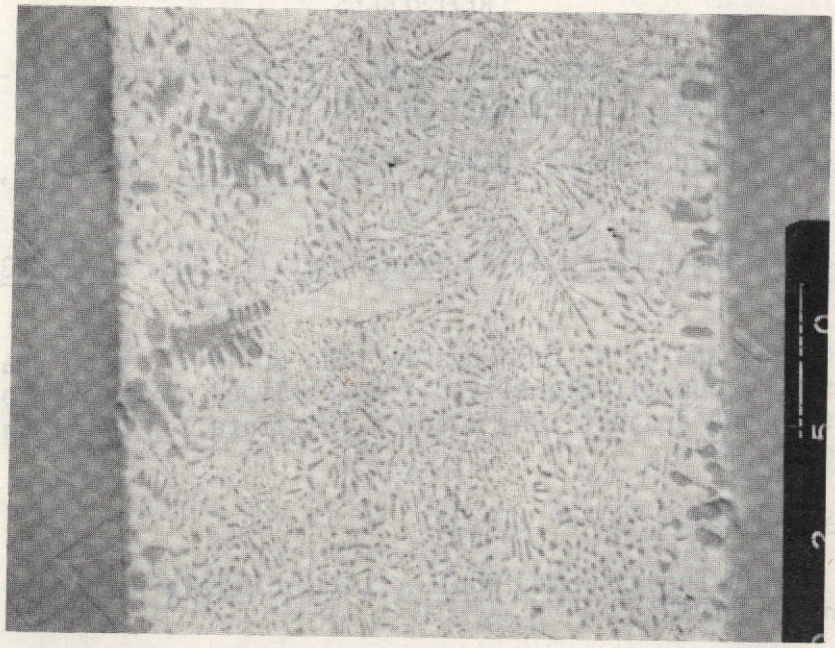

Figure 1. Scanning Electron Micrograph of SLN 4-20mm - 120° showing the two kinds of primary phases. (250X)

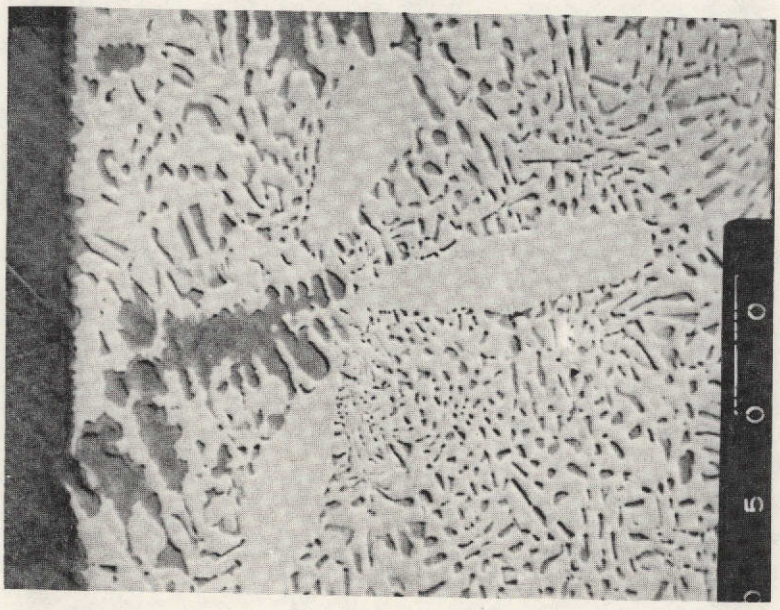

Figure 2. Close-up of the same region shown above. Notice the dark copper phase extending from the nickel surface with three light silver phase regions at its tip. (500X)

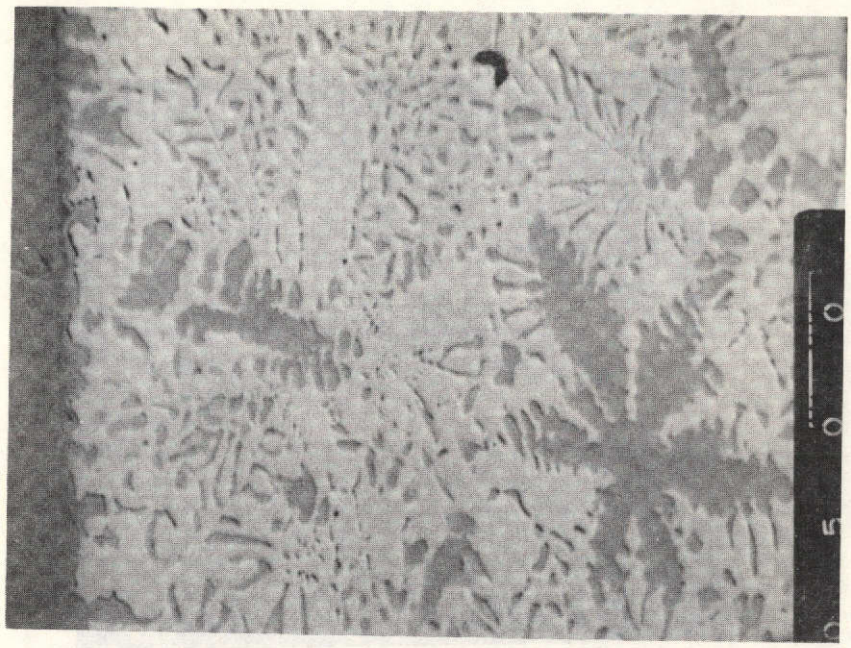

Figure 3. Scanning Electron Micrograph of SLN 4-21mm - 120° showing similar structure to Figures 1 and 2. (500X)

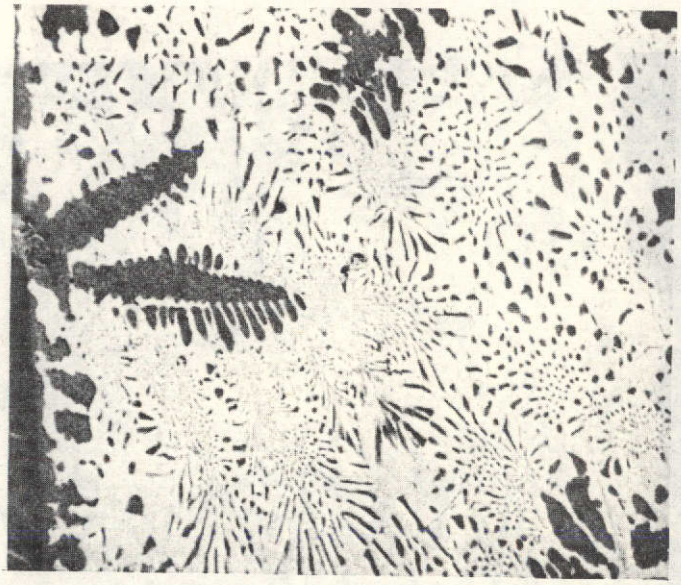

Figure 4. Scanning Electron Micrograph of MCN 6-8mm - 90° showing a typical copper-rich dendrite and copper-rich reaction layer adjacent to the pure nickel at the far left. (500X)

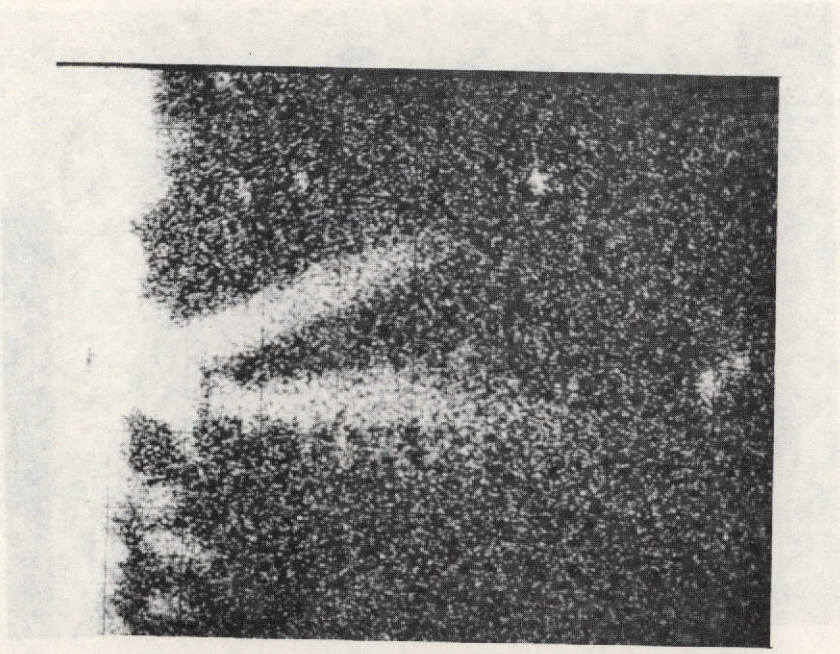

Figure 5. Nickel Kα X-ray scan of the same region as Figure 4. The light areas show the highest nickel concentrations. (500X)

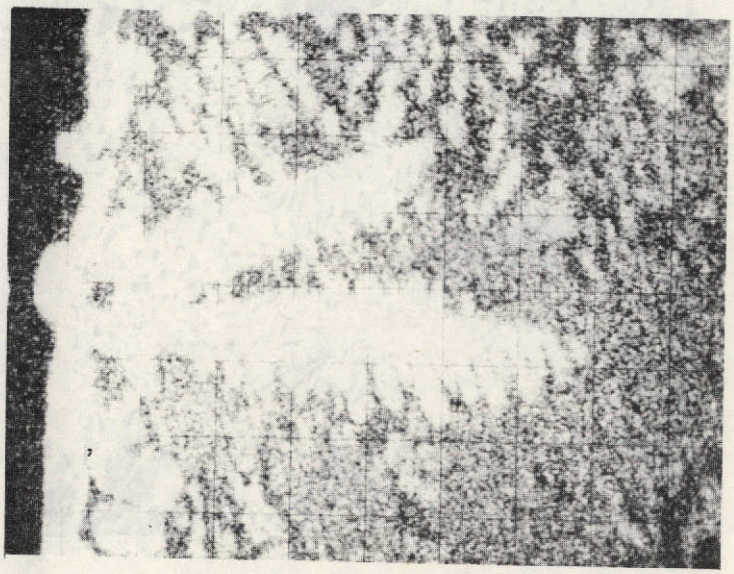

Figure 6. Copper Kα X-ray scan of the same region as Figure 4 (500X)

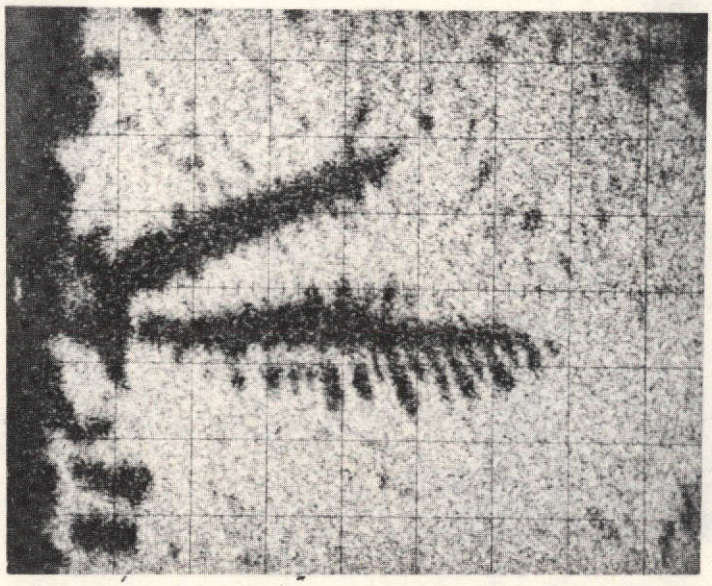

Figure 7. Silver Lα X-ray scan of the same region as Figure 4. (500X)

Figure 8. Scanning Electron Micrograph of SLN 4-5mm - 290° with a large dendrite. (250X)

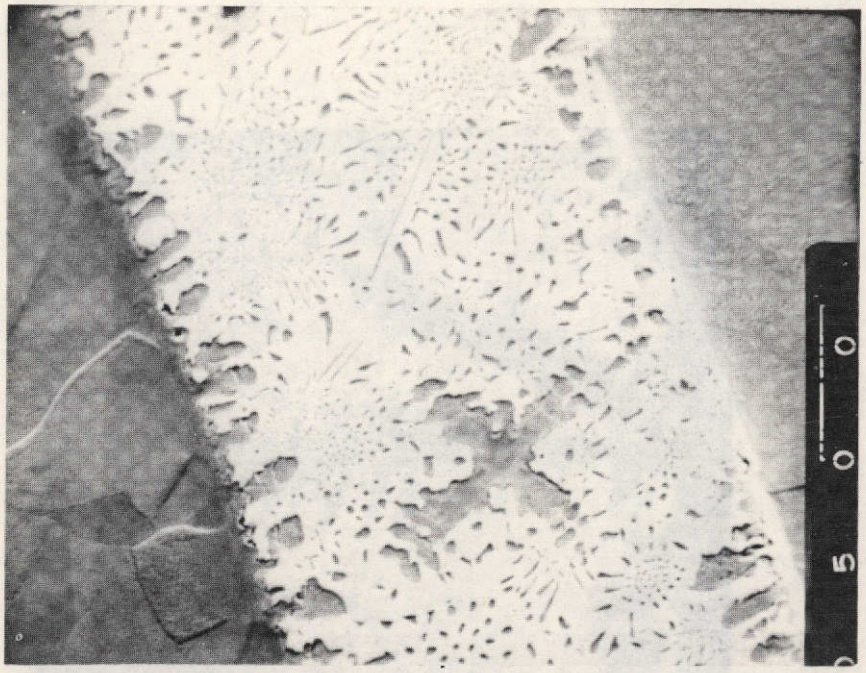

Figure 9. Scanning Electron Micrograph of SLN 4-18 mm - 90° illustrating the normal structure. (500X)

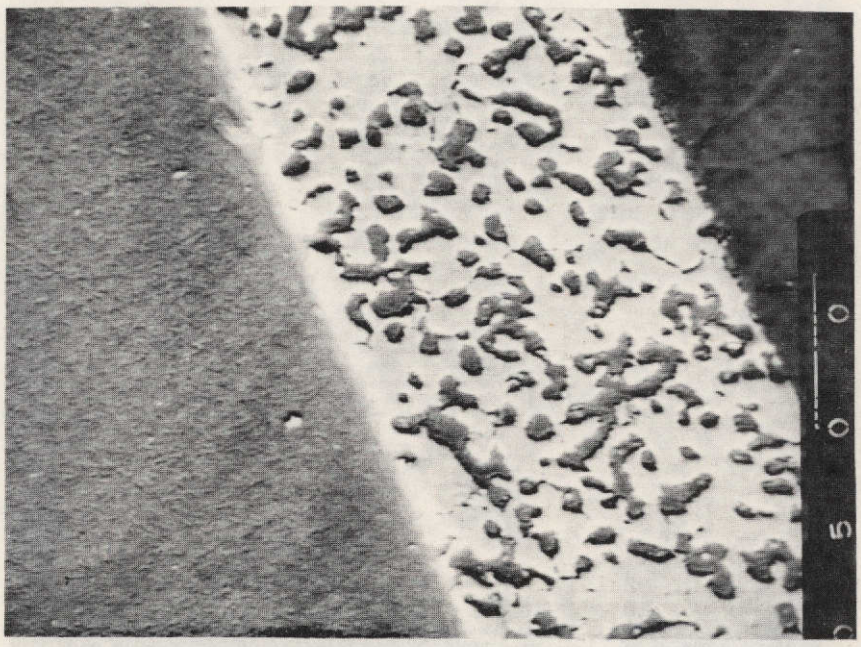

Figure 10. Scanning Electron Micrograph of SLN 4-18mm - 65° illustrating the abnormal structure. (500X)

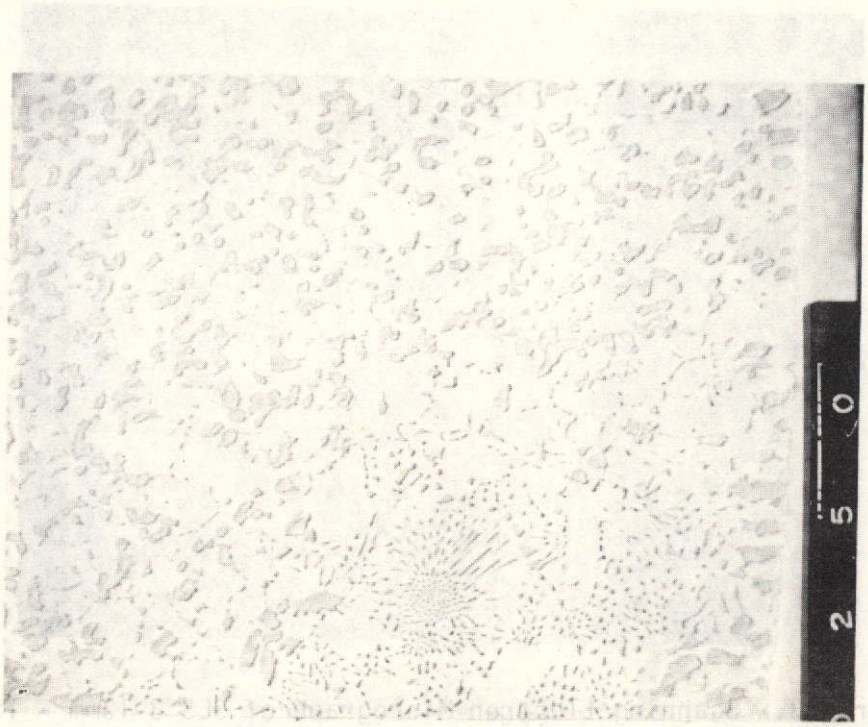

Figure 11. Scanning Electron Micrograph of SLN 4-33mm - 220° illustrating the mixture of normal and abnormal structure in the ring-groove farthest from the zero plane. (250X)

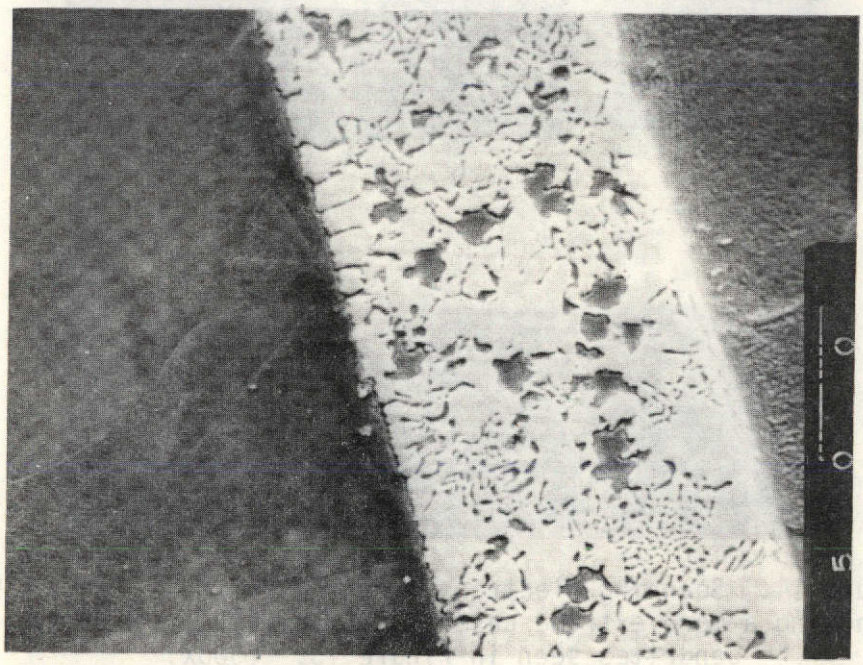

Figure 12. Scanning Electron Micrograph of SLN 4-18mm - 75° illustrating the mixed structure. (500X)

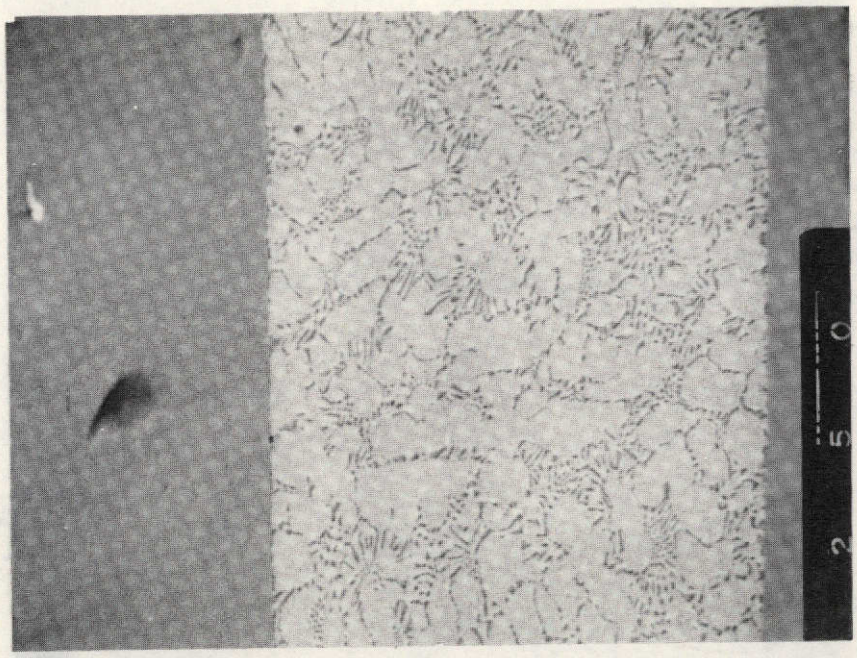

Figure 13. Scanning Electron Micrograph of SLS 3-13mm - 150° showing the primary silver-rich dendrites (large white areas) which were never seen on ground characterizations. (250X)

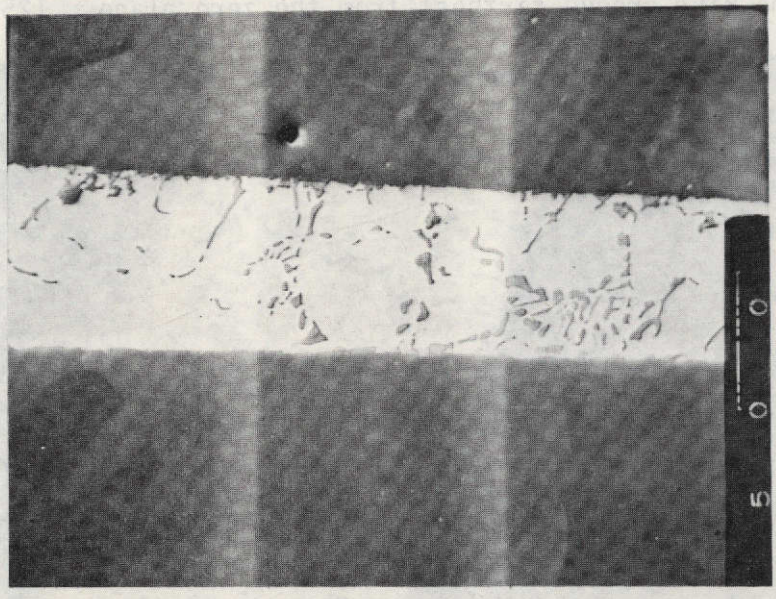

Figure 14. Scanning Electron Micrograph of SLS 3-17mm - 5° showing a more extreme case of the primary silver-rich dendrites seen in Figure 13. (500X)

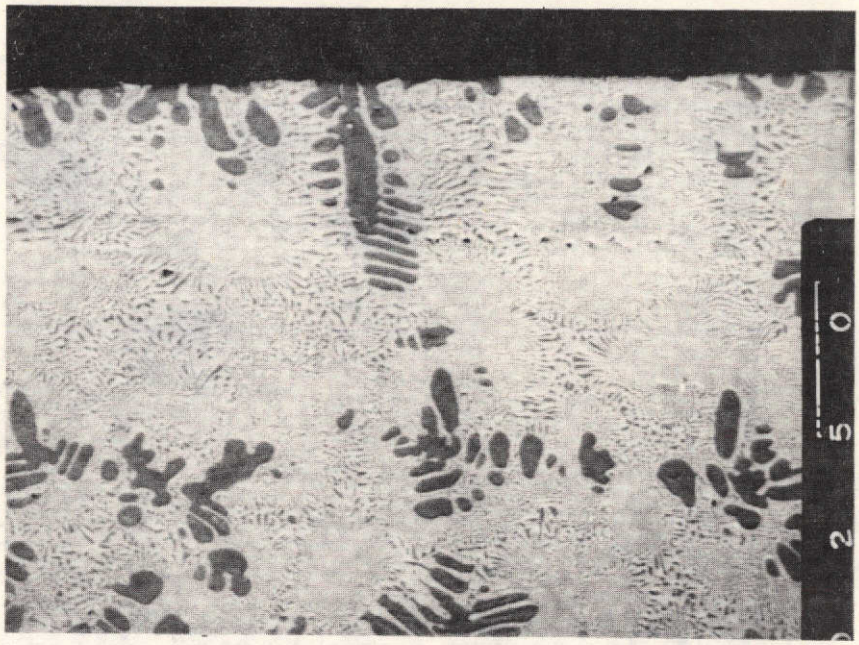

Figure 15. Scanning Electron Micrograph of SLS 3-28mm - 5° showing dendrites present in the ring-groove along with the complete absence of the primary silver phase shown in Figures 13 and 14. (250X)

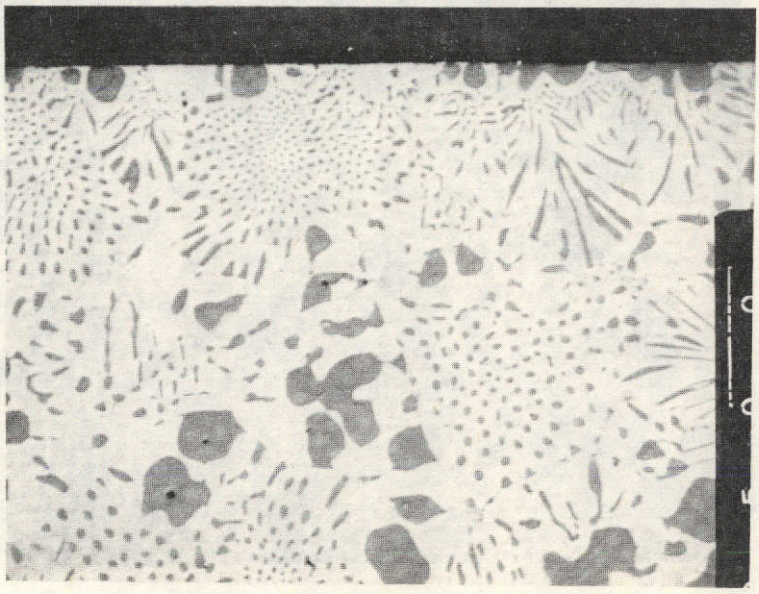

Figure 16. Scanning Electron Micrograph of MCS 6-11.7mm - 260° showing the normal eutectic adjacent to stainless surface (at top). (500X)

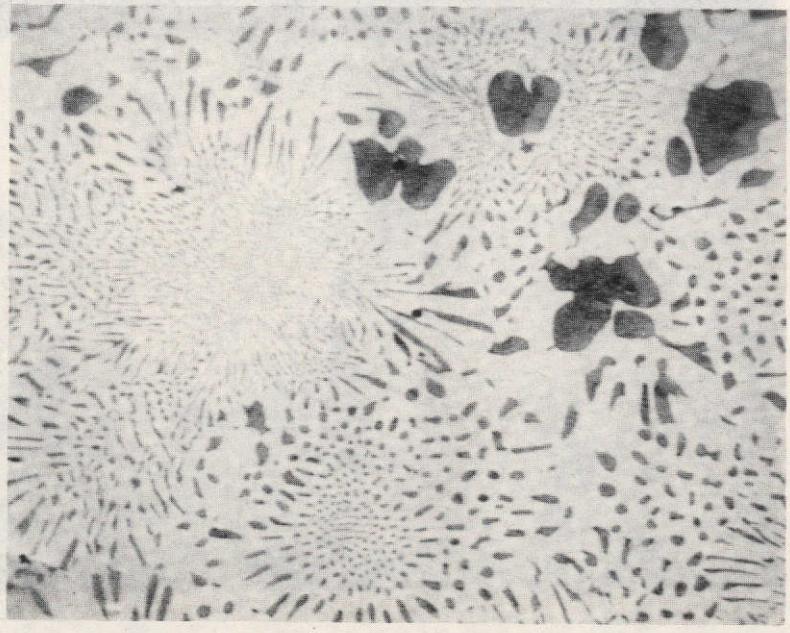

Figure 17. Scanning Electron Micrograph of MCS 6-11.7mm - 280° showing again the ground characterization microstructure. (500X)

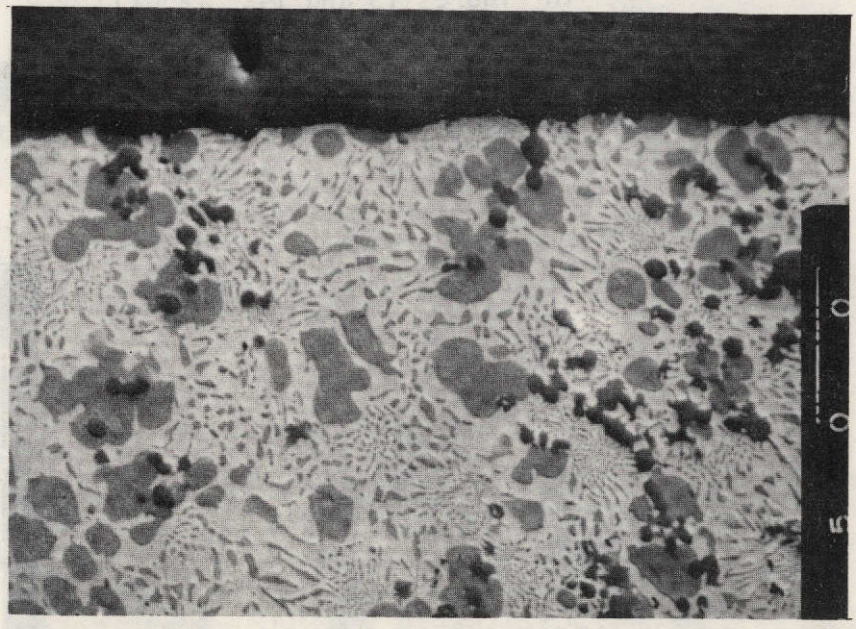

Figure 18. Scanning Electron Micrograph of SLS 3-7mm - 315° showing stainless steel particles near stainless steel-braze alloy interface. (500X)

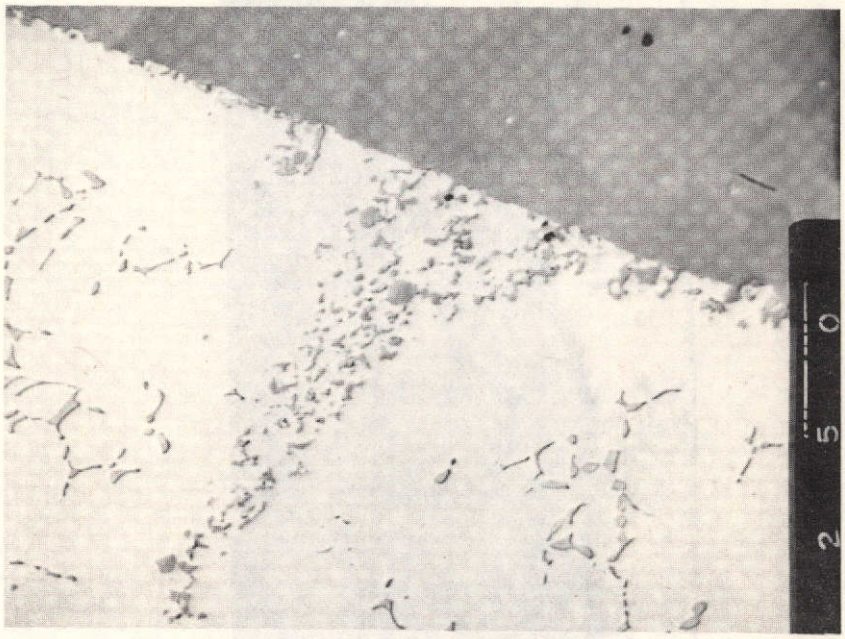

Figure 19. Scanning Electron Micrograph of SLS 3-12mm - 5° showing stainless particles in braze alloy. (500X)

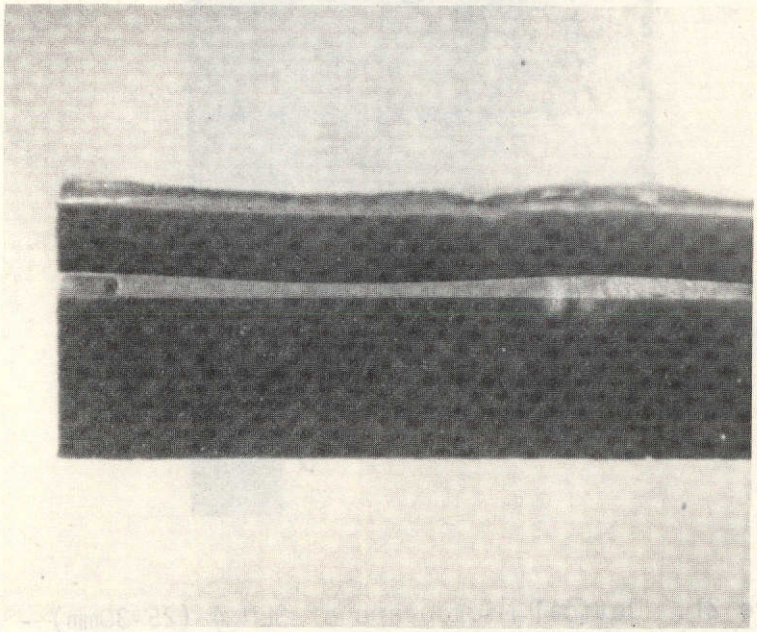

Figure 20. Macrograph of SLS 3-(10-24mm) - 150° showing braze material preferentially at narrowest region of deformed .020" gap (~6X).

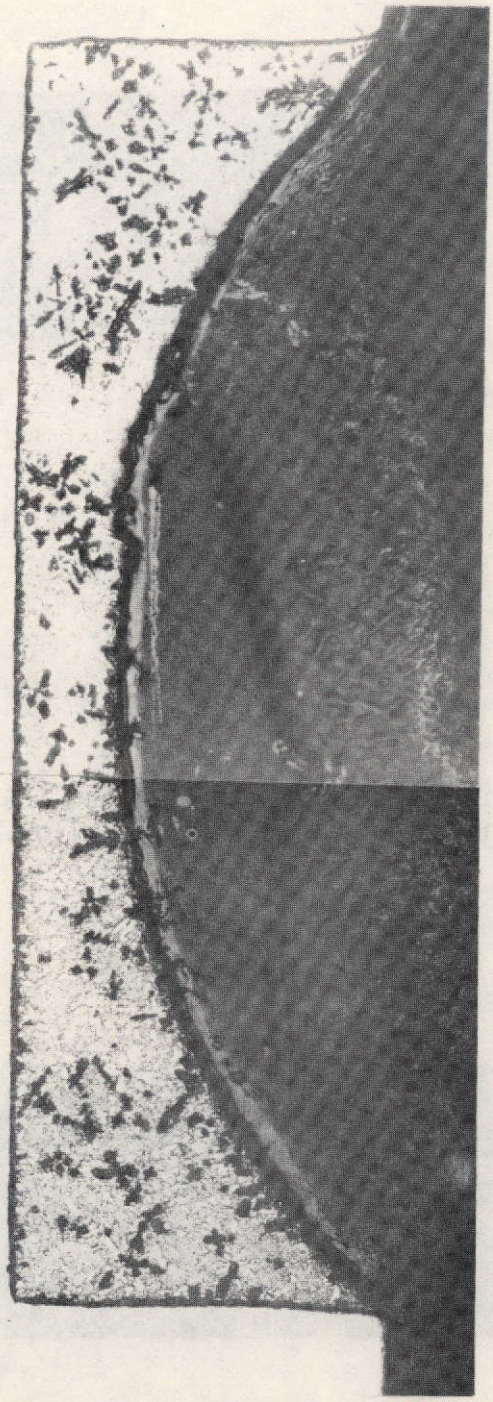

Figure 21. Optical Micrograph of SLN 4-(25-30mm) - 320° showing the microstructure and meniscus in the ring-groove at the wide gap end. (50X)

APPENDIX I

SOLUBILITY OF NICKEL IN LIQUID SILVER-COPPER ALLOY

Study and comparison of Skylab and ground characterization nickel specimens revealed surprising differences in concentrations of nickel in the silver-copper braze alloy. These concentrations were much higher in the Skylab specimens (SLN 2 and SLN 4) than in the ground characterization specimens (MCN 1, 2 and 3 and MCN 4, 5 and 6), and there were consequent dramatic differences in metallographic structure.

One suggestion advanced to explain this difference in nickel concentrations was to the effect that the Skylab specimens may have experienced higher temperatures.

The work of Guertler and Bergmann[1] on the silver-copper-nickel ternary system indicates it would be necessary to reach temperatures in excess of 1250°C to dissolve 8% nickel in the braze alloy. This temperature is more than 250°C higher than expected. While the exothermic heat sources used for the M 552 experiment may not be perfectly reproducible, and it was impossible to measure temperatures during brazing, such vast overheating of the Skylab specimens seems most improbable. Moreover, further interpretation of the Guertler and Bergmann study indicates the solid phase in equilibrium with the saturated silver-copper-nickel liquid would contain 82% nickel; this, in turn, would be reflected in very high local nickel concentrations (in excess of 80%) in the centers of dendrites in the solidified structure, and these have not been found.

The conclusions are (a) Overheating is not a reasonable explanation of the high nickel concentrations found in the braze alloy in the Skylab specimens. (b) Nickel is substantially more soluble in liquid silver-copper alloy than indicated by Guertler and Bergmann. (c) Space may provide an improved environment for the determination of solubilities in certain liquid-solid systems.

APPENDIX II

THERMAL DEFORMATION OF SKYLAB SPECIMENS

Due to mechanical interference during thermal expansion and contraction, there was some deformation of the Skylab specimens.

In the case of the taper-gap nickel skylab specimen (SLN 4), the deformation took place after solidification of the braze alloy. This is revealed in Figures 23 through 26, clearly showing distortion of the capillary gap at various elevations in the specimen. However, the gap clearance where braze alloy has solidified is quite uniform, indi-

cating deformation was subsequent to solidification, and has been confined to those locations not constrained by the solidified braze alloy.

In the case of at least one stainless steel Skylab specimen (SLS 3) this deformation preceded solidification, such that the gap clearance exhibits non-uniformity in locations secured by the solidified braze alloy (Figure 20).

APPENDIX III

CAPILLARY FLOW OF BRAZE ALLOY

Radiographs of all Skylab and ground characterization specimens are shown in Figures 27 through 42, and, taken in aggregate, reveal much about the pattern of the capillary flow under the influences of surface tension and, in the ground characterization specimens, gravity.

Consistently, the braze alloy flows toward locations where the surface tension generates minimum pressures, i.e. where the gap clearance is at a minimum. Thus, the ring grooves tend to be completely drained of braze alloy, when these grooves are located near capillary gaps of small clearance. This is shown quite clearly in Figure 27 which is the stainless steel Skylab specimen with 0.005 inch gap, and also in Figure 39, the taper gap nickel Skylab specimen, where the ring groove near the narrow end of the taper has been exhausted of braze alloy. Also in Figure 39, the other ring groove near the wide portion of the taper gap still retains much of the braze alloy. This tendency for the braze alloy to seek narrow gap locations is also manifested in the wide-gap stainless Skylab specimen (Figure 35). Thermal deformation of this specimen caused variations in gap clearance; the thin gap locations show in this figure as slightly darkened regions centered within patches of braze alloy. The wide gap locations are not occupied by braze alloy, and the ring grooves, adjacent to the relatively wide capillary gap, retain appreciable quantities of braze alloy.

Finally, the influence of gravity predominates only in large gap clearances, as exhibited in the wide-gap stainless ground characterization specimens, shown in Figures 36, 37 and 38; in these specimens the braze alloy has settled downward under the action of gravity.

	Region of Observation in Particle	SLN-4 Skylab	MCN 4,5, & 6 Ground Characterization
Nickel Samples			
Nickel Solubility in Primary Copper Phase			
a) Normal Microstructure see Figures 4 & 9	center	20% Ni	23% Ni
	edge	10% Ni	4% Ni
b) Partially Normal (Mixed) see Figure 12	center	35% Ni	did not occur on ground
			"
c) Abnormal Microstructure see Figure 10	center	37% Ni	did not occur on ground
	edge	24% Ni	"
d) Boundary (Reaction Layer)	adjacent to nickel	34% Ni	22% Ni
	edge	12% Ni	6% Ni
		SLS-3	**MCS 4,5, & 6**
Stainless Steel Samples			
Nickel Solubility in Primary Copper Phase			
a) Ring Groove	center	3% Ni	3% Ni
	edge	.5% Ni	.5% Ni
b) .020" Gap	center	did not occur on Skylab	3% Ni
	edge	"	1% Ni
Bulk Analysis			
a) Ring Groove		28% Cu trace Ni, remainder Ag	26-28% Cu trace Ni, remainder Ag
b) .020" Gap		4.6-7.3% Cu trace Ni, remainder Ag	26-28% Cu trace Ni, remainder Ag

Figure 22. Microprobe Analysis in the Braze Alloy.

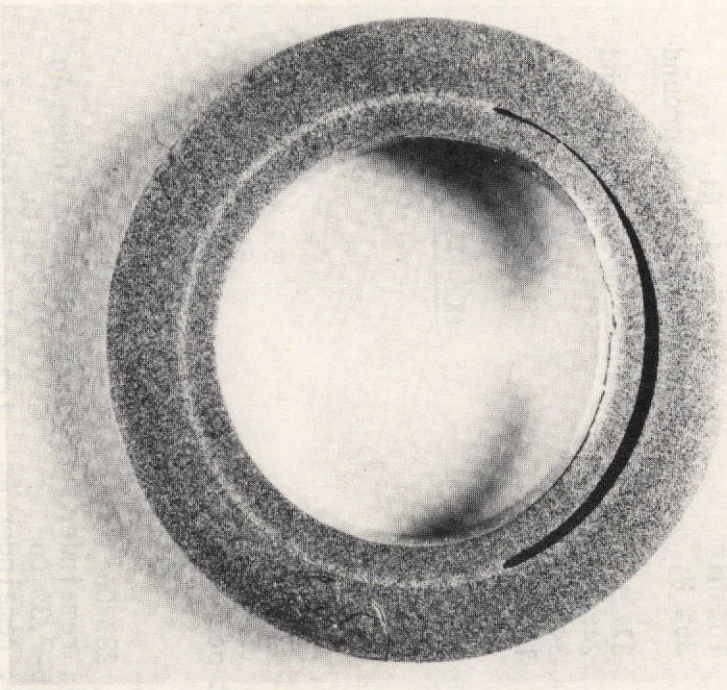

Figure 23. Optical Photograph of SLN-4.7 (21mm) showing deformation in direction of zero plane (approx. 3X).

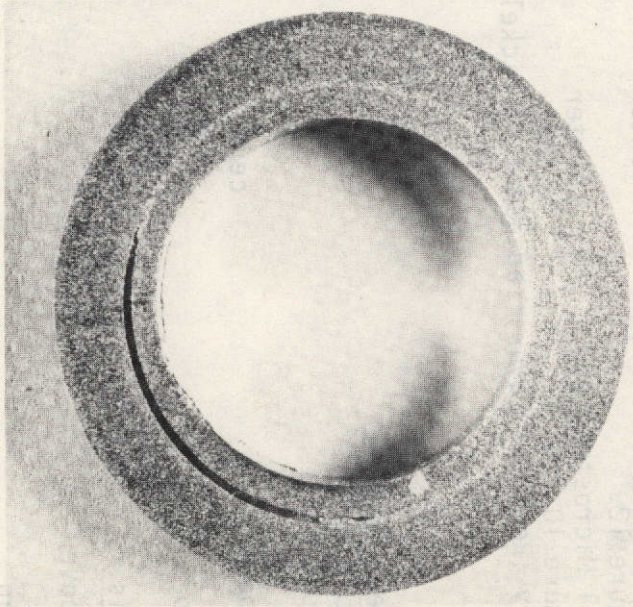

Figure 24. Optical Photograph of SLN-4.8 (21mm) showing deformation in direction opposite zero plane (approx. 3X).

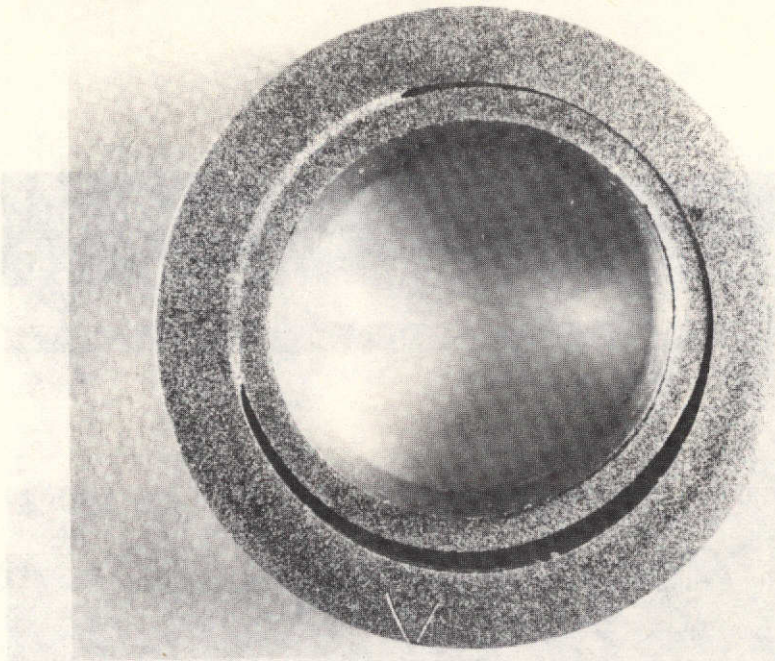

Figure 25. Optical Photograph of SLN-4.8 (24.5 mm) showing deformation in direction of zero plane (approx. 3X).

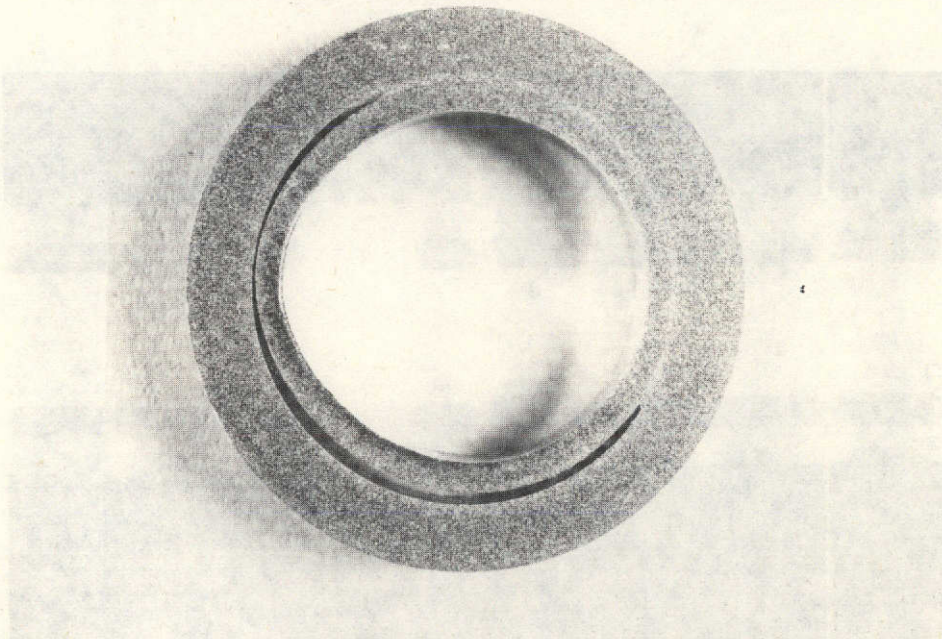

Figure 26. Optical Photograph of SLN-4.9 (24.5mm) showing deformation in direction opposite zero plane (approx. 3X).

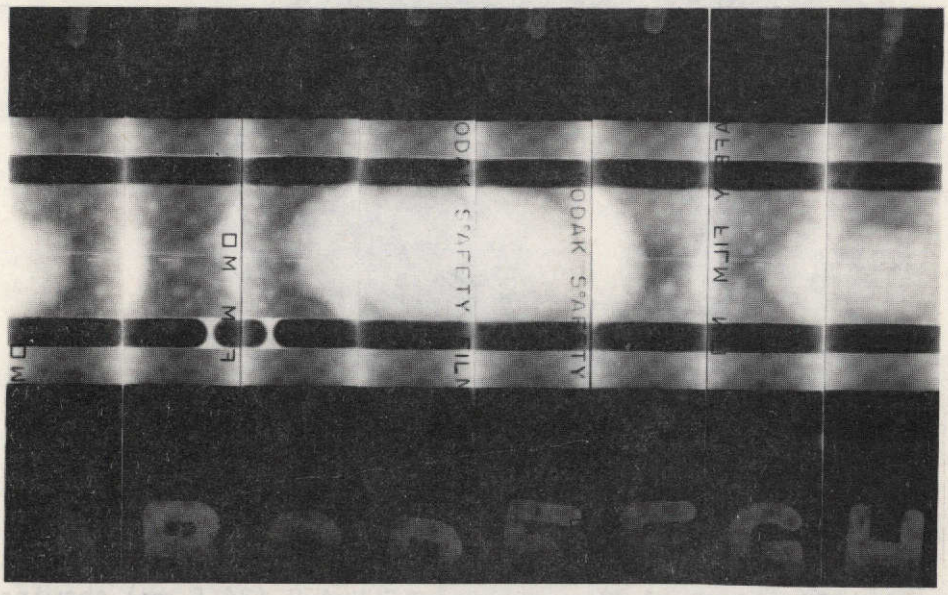

Figure 27. Composite Radiograph of SLS-1 (Skylab Stainless Steel Specimen with .005" gap).

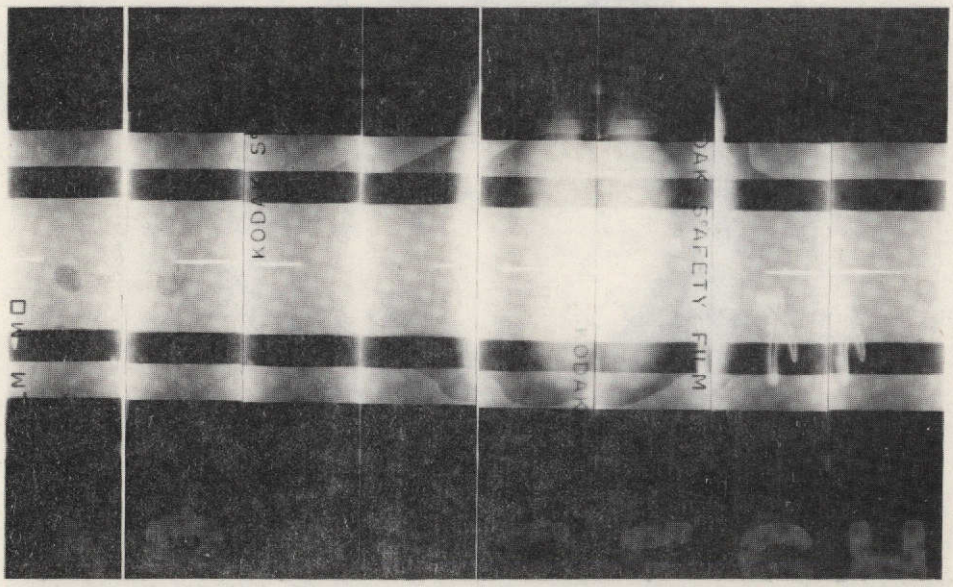

Figure 28. Composite Radiograph of MCS-1 (Ground Characterization Stainless Steel Specimen with .005" gap).

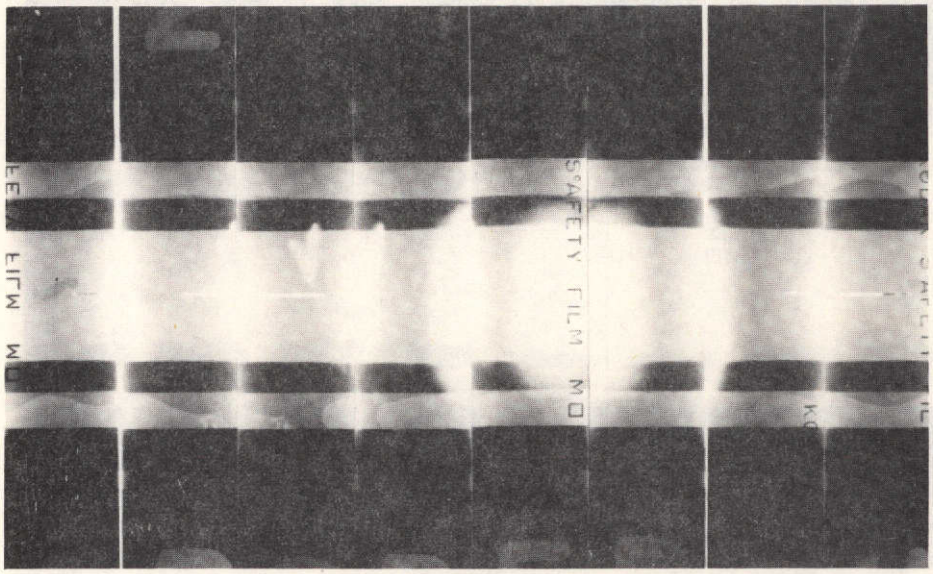

Figure 29. Composite Radiograph of MCS-2 (Ground Characterization Stainless Steel Specimen with .005" gap).

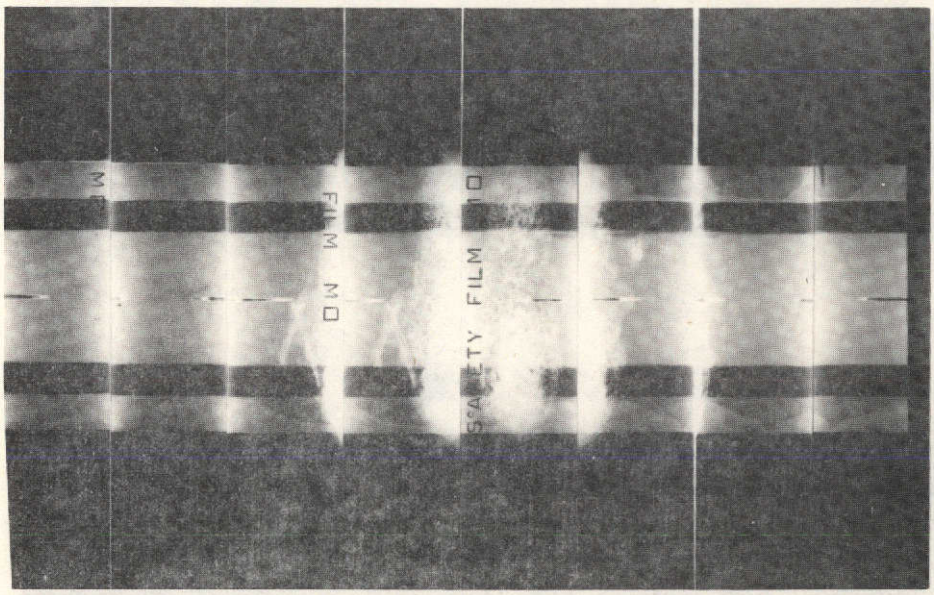

Figure 30. Composite Radiograph of MCS-3 (Ground Characterization Stainless Steel Specimen with .005" gap).

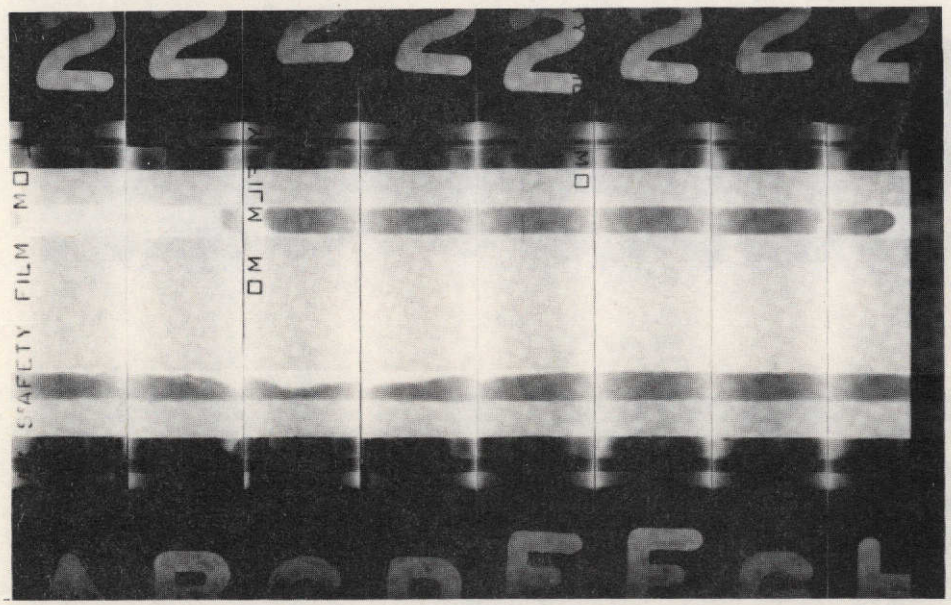

Figure 31. Composite Radiograph of SLN-2 (Skylab Nickel Specimen with .010" gap).

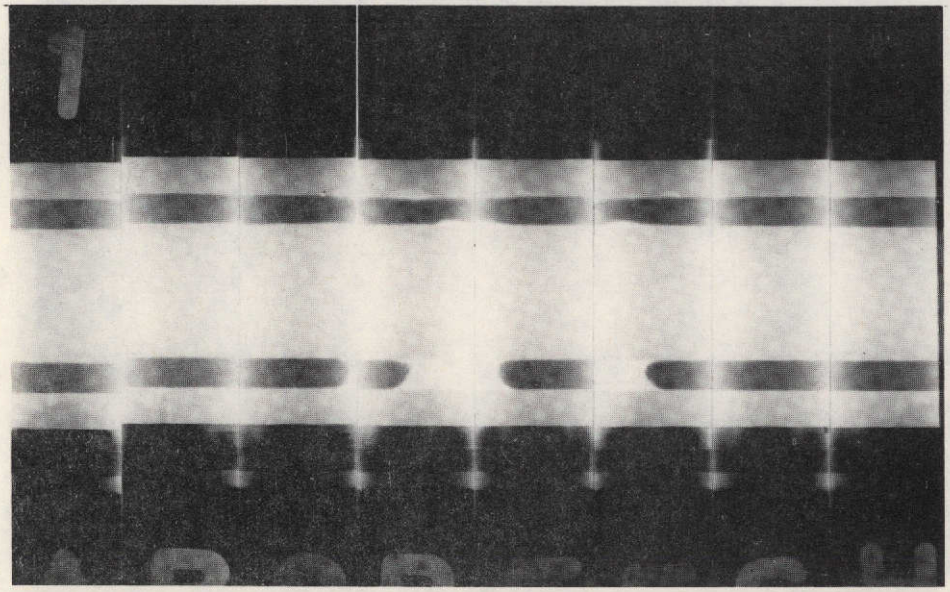

Figure 32. Composite Radiograph of MCN-1 (Ground Characterization Nickel Specimen with .010" gap).

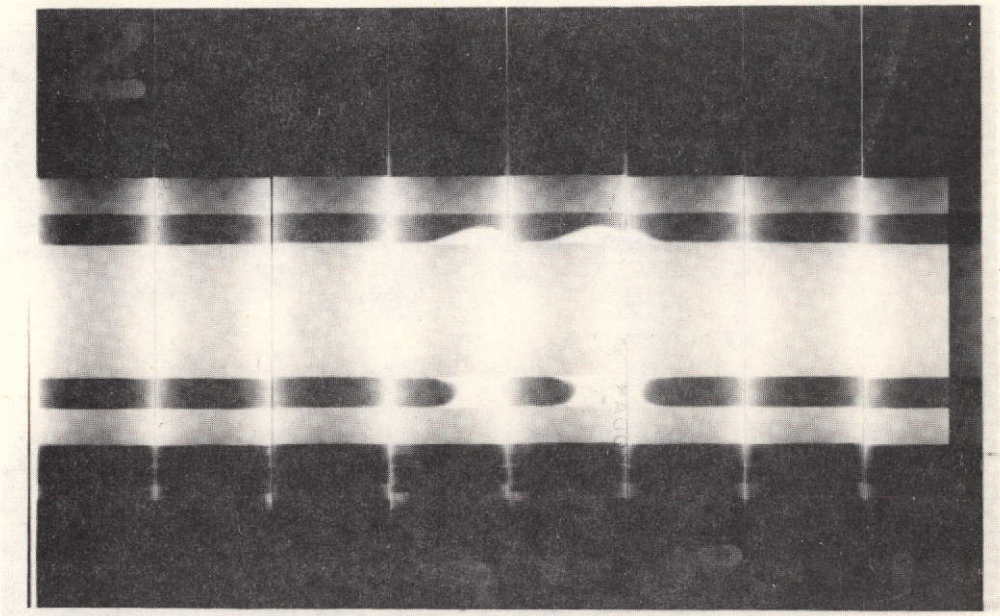

Figure 33. Composite Radiograph of MCN-2 (Ground Characterization Nickel Specimen with .010" gap).

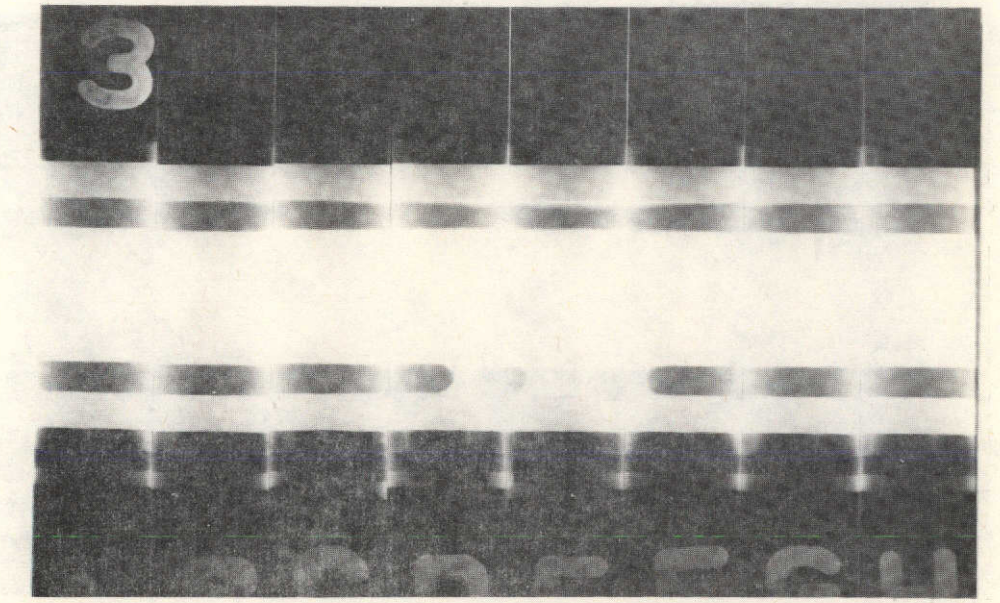

Figure 34. Composite Radiograph of MCN-3 (Ground Characterization Nickel Specimen with .010" gap).

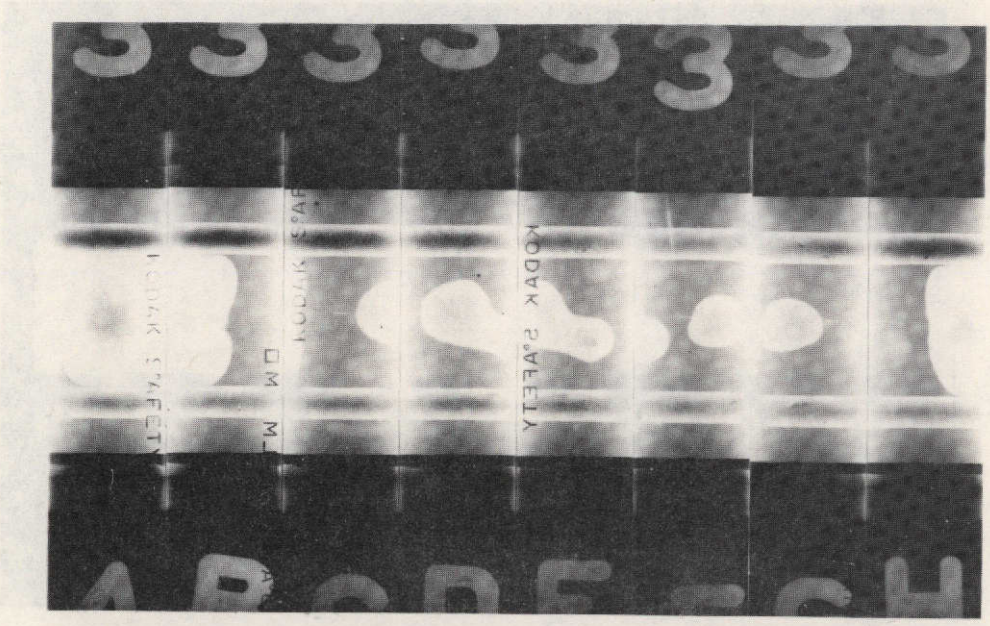

Figure 35. Composite Radiograph of SLS-3 (Skylab Stainless Steel Specimen with .020" gap).

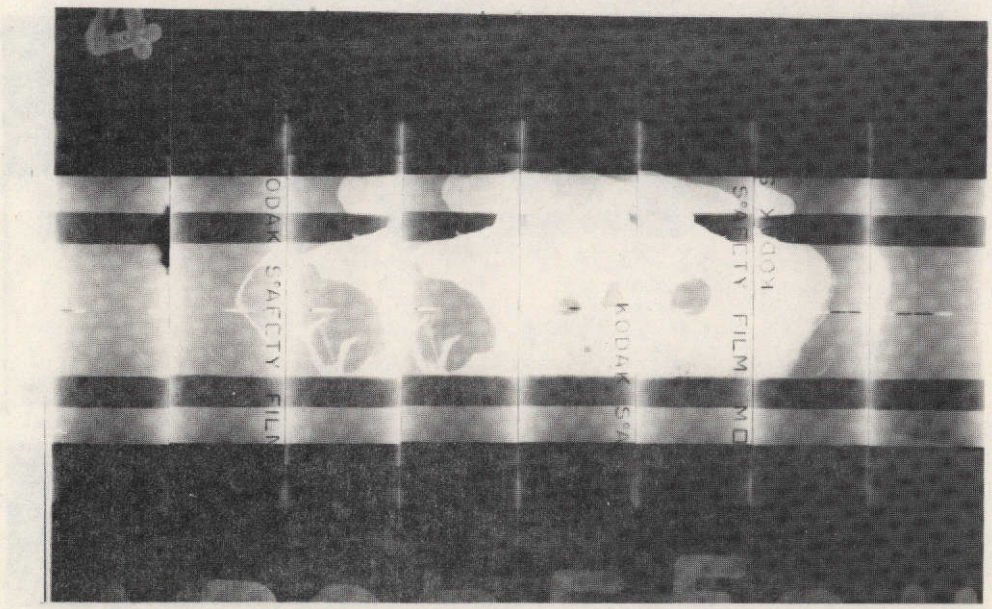

Figure 36. Composite Radiograph of MCS-4 (Ground Characterization Stainless Steel Specimen with .020" gap).

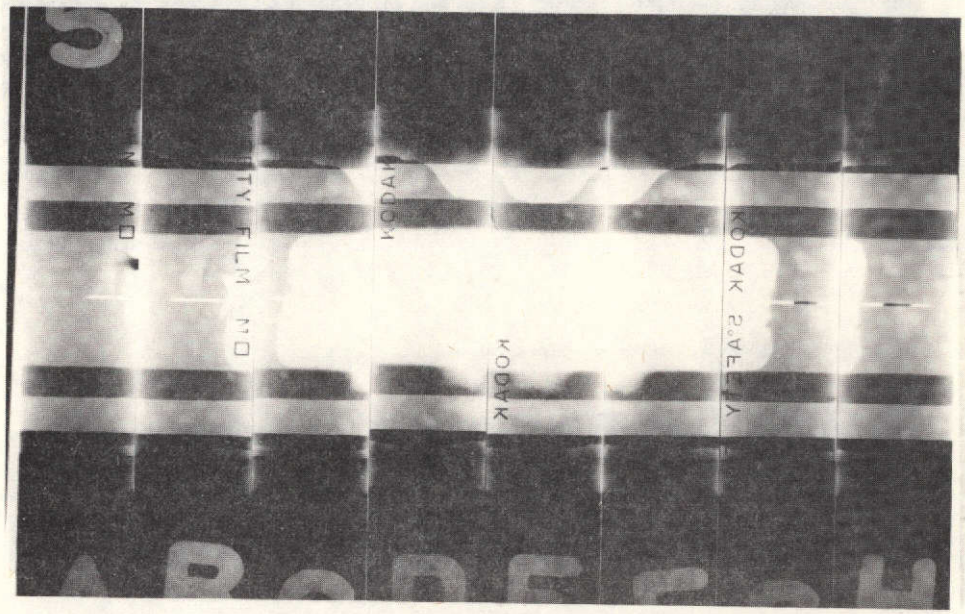

Figure 37. Composite Radiograph of MCS-5 (Ground Characterization Stainless Steel Specimen with .020" gap).

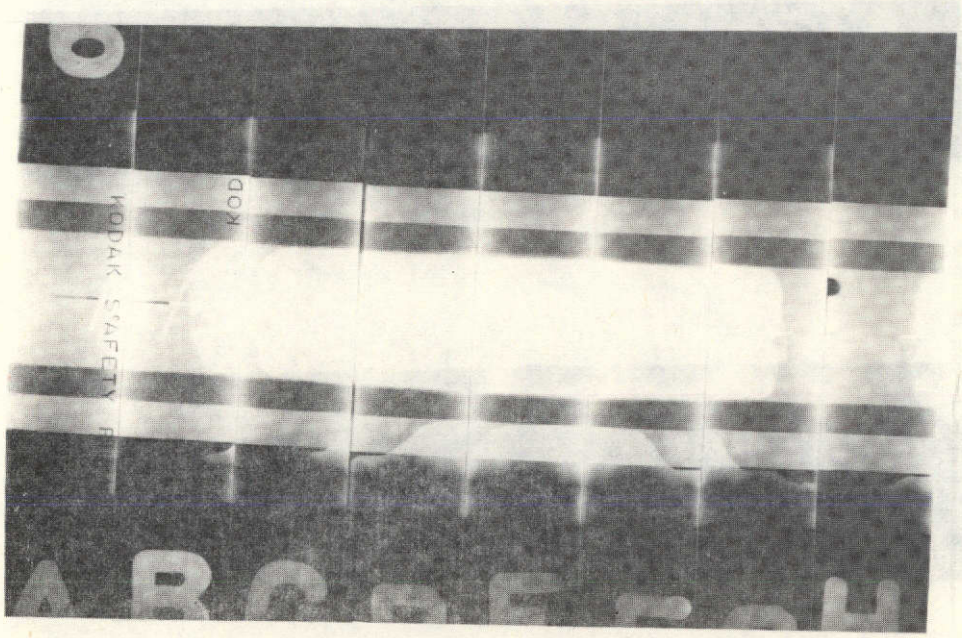

Figure 38. Composite Radiograph of MCS-6 (Ground Characterization Stainless Steel Specimen with .020" gap).

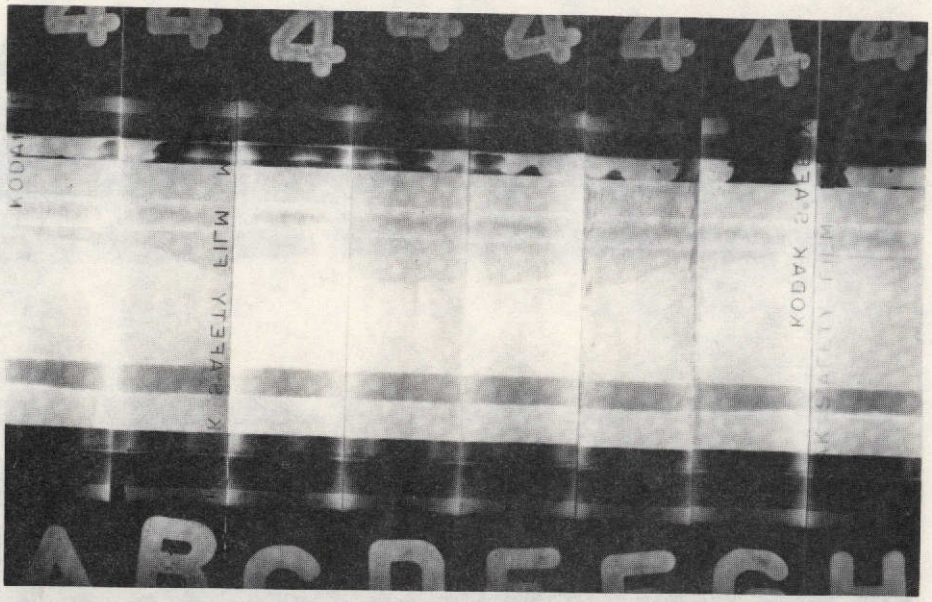

Figure 39. Composite Radiograph of SLN-4 (Skylab Nickel Specimen with 0-.030" gap).

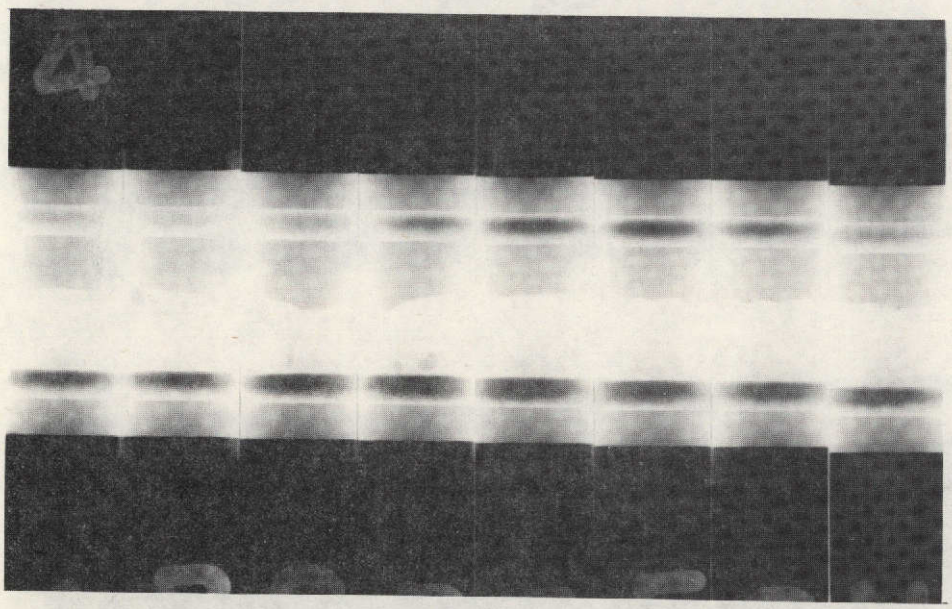

Figure 40. Composite Radiograph of MCN-4 (Ground Characterization Nickel Specimen with 0-.030" gap).

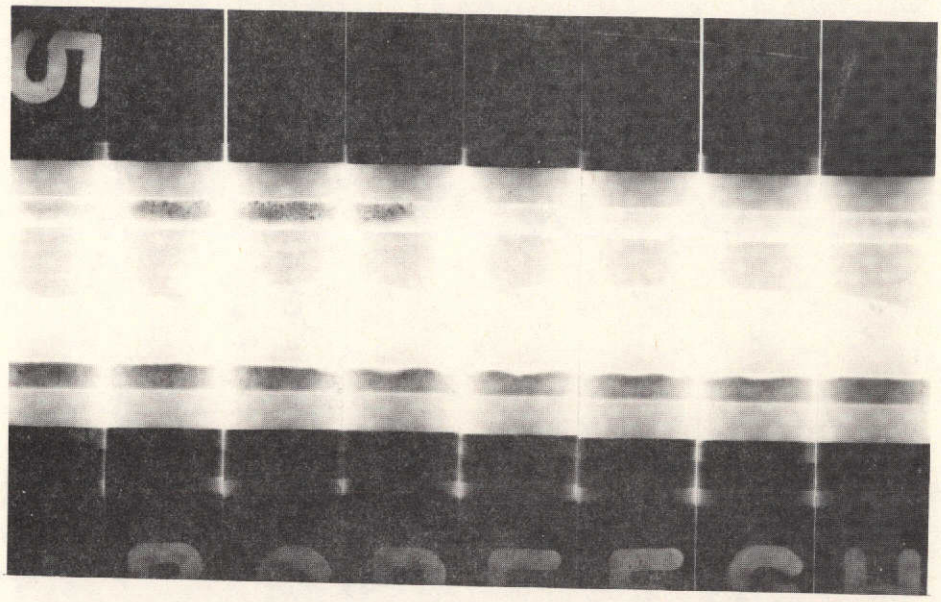

Figure 41. Composite Radiograph of MCN-5 (Ground Characterization Nickel Specimen with 0-.030" gap).

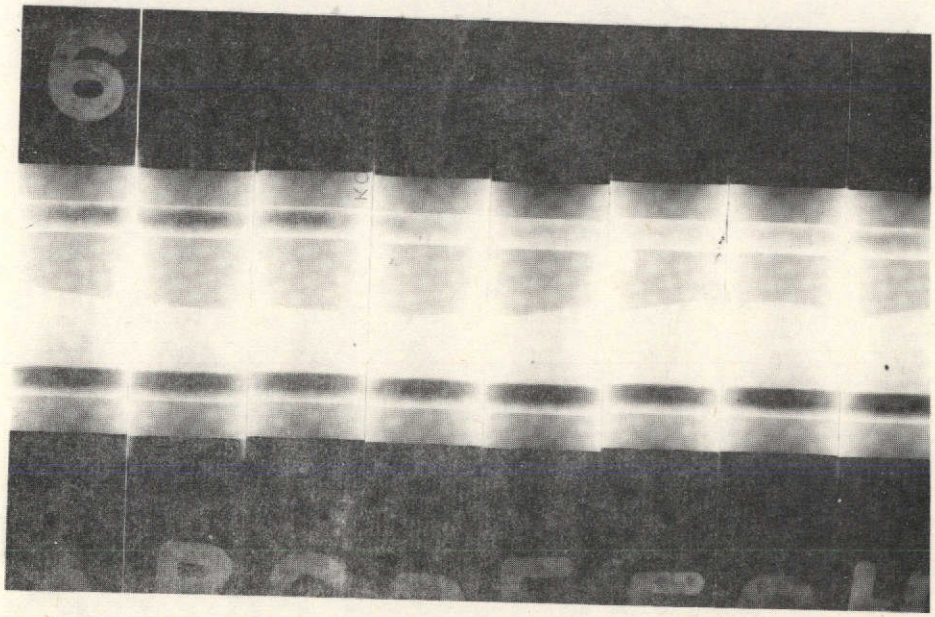

Figure 42. Composite Radiograph of MCN-6 (Ground Characterization Nickel Specimen with 0-.030" gap).